International Journal of Power and Energy Systems, Vol. 42, No. 10, 2022
An Open Access Paper

CFD STUDY OF AN INNOVATIVE SOLAR PHOTOVOLTAIC THERMAL COLLECTOR (PVTC) FOR SIMULTANEOUS GENERATION OF ELECTRICITY AND HOT AIR

Sanjeet Kumar,* Supreme Das,* Agnimitra Biswas,* and Biplab Das*

Abstract

The objective of the present study is to develop an innovative air-based photovoltaic thermal collector (PVTC) and perform a detailed thermal analysis of the same using Ansys Fluent CFD software to improve its efficiency. Rectangular baffles are attached on either side of the thermal absorber having air flow on its both sides. Two different design features of the baffles are considered – baffle length and pitch. The variations of useful heat gain, electrical efficiency, overall efficiency, and air outlet temperature are modelled for a characteristic solar day. It is shown that the present PVTC achieves the maximum overall efficiency of 44.44% for a baffle length of 44 mm and pitch of 60 mm. The flow physics is then investigated to understand the heat transfer augmentation between the baffles with different pitch lengths. Finally, usefulness of the PVTC is shown by comparing its performance with a few established designs of the literature.

Key Words

Photovoltaic thermal collector (PVTC), baffle length, pitch length, electrical efficiency, thermal efficiency, overall efficiency

1. Introduction

A hybrid photovoltaic thermal collector (PVTC) converts incident solar energy partly into electrical energy with the help of photovoltaic cell and partly into thermal energy with the help of the thermal collector. Mojumder *et al.* [1] performed an experimental study on unglazed PVTC with fins. Effect of number of fins and mass flow rate of air was highlighted. Results indicated that the collector with four fins provided maximum thermal and PV efficiency. Performance comparison of semi-transparent PVTC with PVTC integrated with a thermoelectric cooler was made by Dimri *et al.* [2]. The electrical and thermal exergy gain of the new system was higher than that of the semi-transparent PVT air collector. Slimani-El *et al.* [3] modelled the heat transfer and energy performance of a PVTC with double-pass air flow. Performances of three different PVTC designs were compared for the climatic condition of Algeria [4], revealing that the daily average energy efficiency of double-pass PVTC was higher than the remaining three configurations. From the above literature review, it is found that performance of the PVTC or simple solar thermal air collector is improved by various means, *e.g.* through multi-pass, using nanofluids, changing air collector dimensions, using different absorber materials, *etc.*

Thermal performance of the collector has also been increased by using fins [1], [5]–[7]. Velmurugan and Kalaivanan [5] evaluated thermal performance of a double- and triple-pass solar air heater with longitudinal fins and reported better thermal performance of the solar air heater with fins and using triple pass. Velmurugan and Kalaivanan [6] again performed energy and exergy analysis of a single-/dual-pass roughened (with wire-mesh structure) and finned plate solar air heater. Pandey *et al.* [8] designed multiple arc-shaped roughness elements on a absorber plate and investigated their effects on thermo-hydraulic performance of a solar air heater with regard to different gap width ratios. Their novel design improved collector performance compared with the plain absorber plate. Abuşka *et al.* [9] attempted to improve the performance of solar air collector using the conical spring structure on the absorber plate surface and reported enhancement of its performance.

1.1 Research Gap and Objective

Pertinent literatures reveal that thermal performance of the PVTC in the presence of baffle attached on the absorber plate has still not been paid much attention [1], [4]–[14], [15]. But, dimensions of these connectors or baffle plates were not properly estimated. Hence, in this work, an attempt has been made to study the effects of different dimensions of rectangular baffle plates on the thermal

* Department of Mechanical Engineering, National Institute of Technology Silchar, 788010, India; e-mail: {sanjeet.kumar.nits, supremedas.19031987, biplab.2kmech}@gmail.com, agnibis@yahoo.co.in
Corresponding author: Agnimitra Biswas
Recommended by Prof. Ikhlaq Hussain
(DOI: 10.2316/J.2022.203-0383)

performance of an innovative air-based PVTC with the help of Ansys Fluent CFD software. Two design parameters of the baffle plate, *i.e.* baffle length and pitch, have been considered to improve the efficiency of the collector. The purpose is to enumerate their optimal values for higher performance. Further, the flow physics is also investigated.

2. Problem Definition

Two-dimensional CFD simulations are done for this as the three-dimensional effect, *i.e.* width of the baffle on the PVTC performance, is neglected, which will be valid when the flow is predominantly unidirectional (considered in this work).

2.1 Mathematical Formulation

For the photovoltaic module, the energy balance equation can be written as [16]:

$$\tau_g[\alpha_c\beta + \alpha_T(1-\beta)]I(t)bdx = [U_t(T_c - T_a) + U_b(T_c - T_{bs})]bdx + \eta_c\tau_g\beta I(t)bdx \quad (1)$$

For the back surface, the energy balance equation is represented as [16], [17]:

$$U_b(T_c - T_{bs})bdx = h(T_{bs} - T_f)bdx \quad (2)$$

For air flowing below the Tedlar [16]:

$$\dot{m}_f C_a \frac{dT_f}{dx}dX + U_b(T_f - T_a)bdx = h_T(T_{bs} - T_f)bdx \quad (3)$$

The rate of useful energy gain can be calculated for the PVTC system as:

$$Q = \dot{m}_f C_a[T_{air,out} - T_{air,in}] \quad (4)$$

Thermal efficiency of PVTC collector can be evaluated as [16], [18]:

$$\eta_{th} = \frac{\sum Q}{\sum I(t)bL_1} \quad (5)$$

The electrical efficiency of a PV module can be calculated using the following equation as given in [18]:

$$\eta_E = \eta_c[1 - 0.0045(T_c - 298)] \quad (6)$$

The electrical efficiency can be converted into equivalent thermal efficiency through the following equation [18]:

$$\eta_{Eth} = \frac{\eta_E}{C_f} \quad (7)$$

where C_f is a conversion factor, whose value is taken as 0.36 for country like India.

Thus, the overall efficiency of the PVTC can be computed by using the following equation [16], [18]:

$$\eta_o = \eta_{Eth} + \eta_{th} \quad (8)$$

3. CFD Modelling

In this study, the simulation was performed by using Ansys Fluent CFD software.

3.1 Geometrical Modelling of the PVTC

The two-dimensional computational domain of the PVTC system was modelled using an ANSYS geometrical modelling tool. The physical domain is shown in Fig. 1, and Table 1 [16] shows the geometrical dimensions of the PVTC. Figure 1(a) shows the rectangular baffles above and below the thermal absorber. The absorber plate of the thermal collector has a conventional polycrystalline c-Si PV panel draped on its top surface to form the PVTC. A total of 15 pairs of baffles have been constructed, which are accommodated within the length of the absorber plate. The various zones of the PVTC have also been marked. The air flow on top and bottom of the absorber plate (double pass) is also shown. The inlet and the outlet and the other zones are also shown. The various energy interactions in the PVTC along with the double pass of air are shown in Fig. 1(b). It shows different heat transfers that take place in the present PVTC. In the bottom pass, the necessary hear transfer occurs between the heated absorber plate and the fluid.

3.2 Mesh Generation

After the geometrical modelling, hexahedral element of fine size was selected. High relevance centre, smoothing high, and patch conforming technique were used during the generation of the grid to achieve a good quality mesh. Orthogonality condition and aspect ratio were considered for obtaining quality mesh for the simulation. The final computational mesh of the domain is shown in Fig. 2. Grid generation setting used in the present simulation is shown in Table 2.

3.3 Boundary Conditions

Appropriate boundary conditions were applied in the computational domain as per the physics of the problem. Velocity inlet condition was applied at inlet on the left boundary (top of absorber plate, Fig. 1). Similarly, pressure outlet boundary condition was applied at outlet on the left boundary (bottom of absorber plate, Fig. 1). The boundary condition, intensity of solar radiation, was applied to the top surface of the glass. No-slip condition was applied on the baffles and on the absorber plate. The bottom wall (above insulation zone) and the side wall (curved wall) of the PVTC system were defined as non-penetrating wall with zero heat flux condition. The material's thermophysical properties are shown in Table 3.

3.4 Grid Independency Test

For making the computational analysis free from grid effects, grid independence test was carried out for different number of elements. Table 4 shows the levels considered for grid independence for this study. Figure 3 shows the variation of cell temperature with respect to a number of elements. It seems that the seventh refinement level with element number 302569 results in grid independence of the results; hence, this mesh configuration was selected for further simulations.

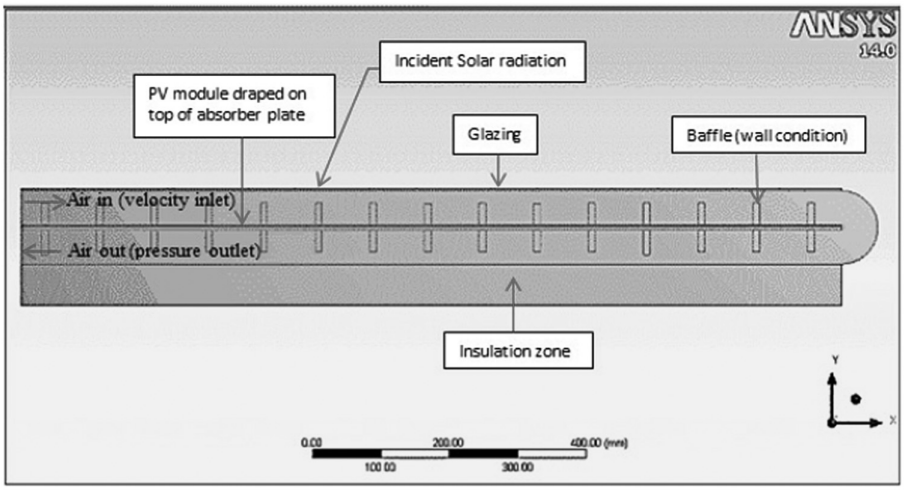

(a)

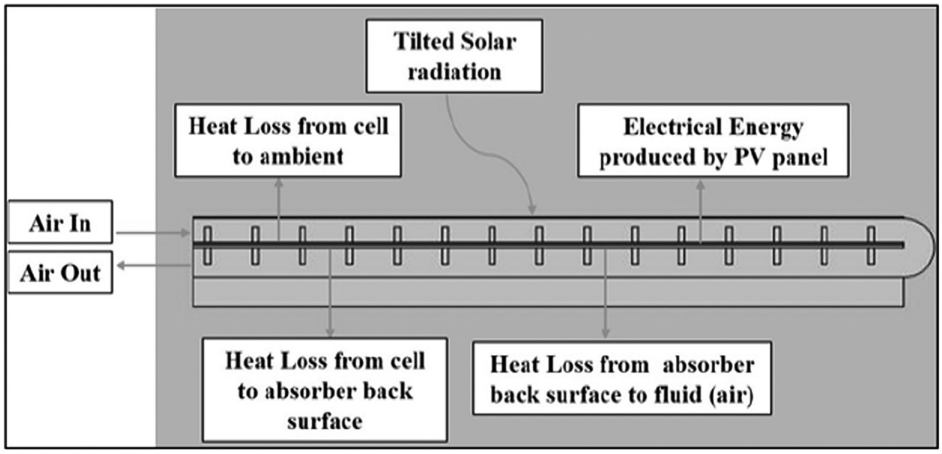

(b)

Figure 1. Geometrical modelling of PVTC in an Ansys design modeller and (b) schematic of the model showing energy interactions.

Table 1
Geometrical Dimensions of the PVTC

Name	Dimensions in m (L × W × T)
Glass	1.2 × 0.45 × 0.003
EVA	1.2 × 0.45 × 0.0005
Absorber plate	1.2 × 0.45 × 0.005
PV cell	1.2 × 0.45 × 0.0003
Tedlar	1.2 × 0.45 × 0.0005
Fluid domain	1.2 × 0.45 × 0.05
Insulation	1.2 × 0.45 × 0.05

4. Results and Discussion

By using CFD simulations, the effects of two design parameters *i.e.* baffle length and baffle pitch length are discussed on the electrical and overall performances of the collector, including outlet air temperature and useful heat gain variations between 8 am and 5 pm. These values are calculated by using the mathematical formulae discussed earlier. Before that the variations of monthly average hourly global solar radiation are shown in Fig. 4 for a city named Silchar in India. It can be seen that the intensity of solar radiation of the place of study peaks around the noon time.

4.1 Useful Heat Gain (W) Variation with Time (hour)

Figure 5(a–c) shows the variations of useful heat gain by the PVTC with time for baffle lengths 36, 40, and 44 mm, respectively, when the pitch length is varied from 60 to100 mm. The useful heat gain increases with the passage of time from morning till noon and then decreases in the afternoon, which is irrespective of any pitch or baffle length. This is the result of the increase of air outlet temperature for a given inlet or ambient temperature. This follows the same trend as the literature results of [19], [20]. Notwithstanding the time frame or the baffle length, the useful heat gains are higher for pitch length of 60 mm due to higher air outlet temperature that results in a larger temperature difference between outlet and inlet of the collector. And with the increase of baffle length from 36 to 44 mm, the useful heat gain increases since the

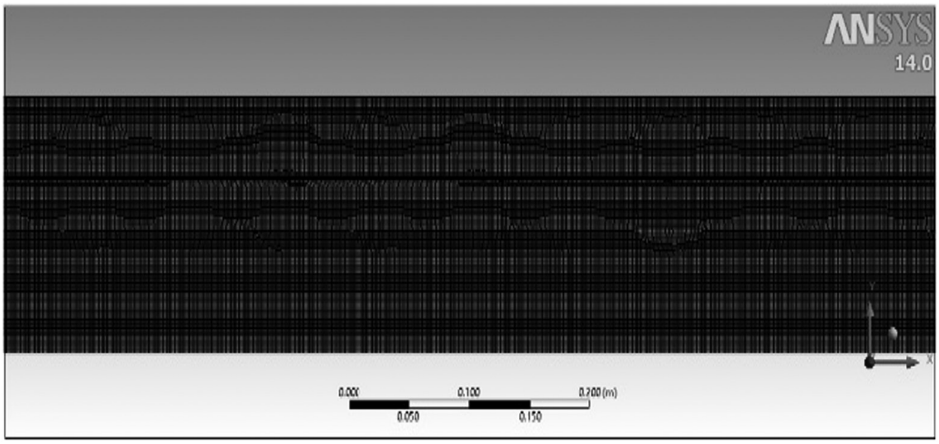

Figure 2. 2D grid generation of PVTC.

Table 2
Grid Generation Setting

Name	Value
Element	Hexahedral
Method	Patch conforming
Relevance centre	Fine

Table 3
Material Properties Used in CFD Analysis [15]–[19]

Material	Thermal Conductivity (W/mK)	Heat Transfer Coefficient (W/m^2K)	Density (kg/m^3)
Glass	1.0	66	2,450
PV cell	0.039	2.8	950
EVA	0.35	0.62	940
Tedlar	0.033	8.11	1,200

outlet air temperature also increases with increase of baffle length. Also, the reason for increase of useful heat gain is the result of increased heat transfer area with increased baffle length. The maximum useful heat gain increases from 33.43 to 35.36 W with baffle length increasing from 36 to 44 mm.

4.2 Electrical Efficiency (%) Variation with Time (hour)

Figure 6(a–c) shows the variations of electrical efficiency with time for different pitch lengths of 60, 80, and 100 mm, respectively, when the baffle length is varied from 36 to 44 mm. These graphs are in the inverted form and follow the same trend as some of the existing literature, *e.g.* [17], [18], [20]. From the graphs, it can be observed that with the passage of time, the efficiency decreases (*i.e.* cell temperature increases) due to the rise of solar

Table 4
Grid Independence Test for Cell Temperature

Sl. No.	No. of Elements	Outlet Air Temperature	Cell Temperature (K)
1	25,264	315.79	315.87
2	52,672	315.64	315.73
3	78,579	315.58	315.68
4	102,760	315.53	315.61
5	152,675	315.44	315.60
6	216,364	315.44	315.60
7	302,569	315.44	315.60

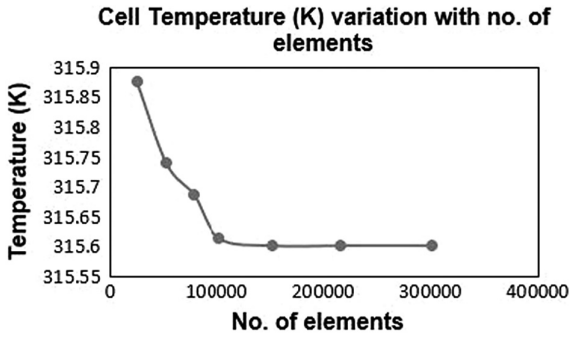

Figure 3. Grid independence test for cell temperature with number of elements.

irradiation up to around forenoon time and after that the same increases due to the decrease in cell temperature during afternoon. The same is irrespective of any pitch length and baffle length. Notwithstanding the time frame, the efficiency is higher for a baffle length of 36 mm. And with the increase of pitch length from 60 to 100 mm, the electrical efficiency also increases. The maximum electrical efficiency increases from 11.49% to 11.51% when pitch length increases from 60 to 100 mm for a fixed baffle length of 36 mm. This is because electrical efficiency

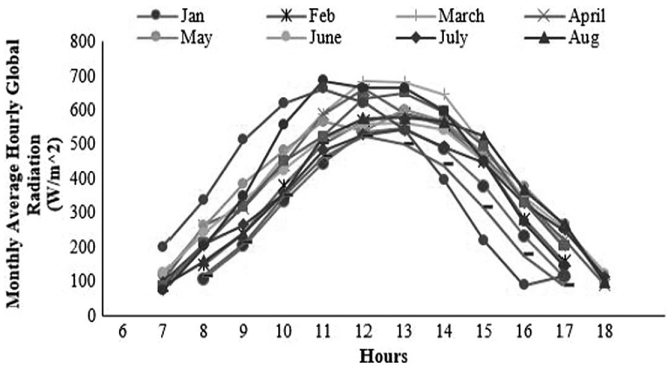

Figure 4. Monthly average hourly global solar radiation.

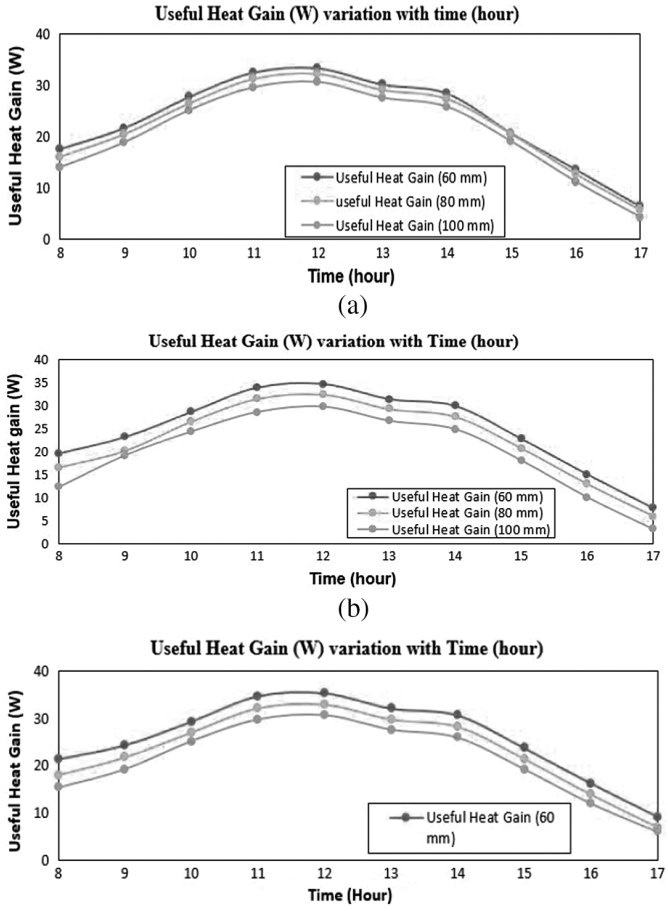

Figure 5. (a) Useful heat gain (W) variation with time (hour) when fixed baffle length ($L = 36$ mm) and varying pitch length (d) 60, 80, and 100 mm; (b) useful heat gain (W) variation with time (hour) when fixed baffle length ($L = 40$ mm) and varying pitch length (d) 60, 80, and 100 mm; and (c) useful heat gain (W) variation with time (hour) when fixed baffle length ($L = 44$ mm) and varying pitch length (d) 60, 80, and 100 mm.

is reduced with an increase in cell temperature and cell temperature variation follows the same trend as useful heat gain, thermal efficiency, and overall efficiency.

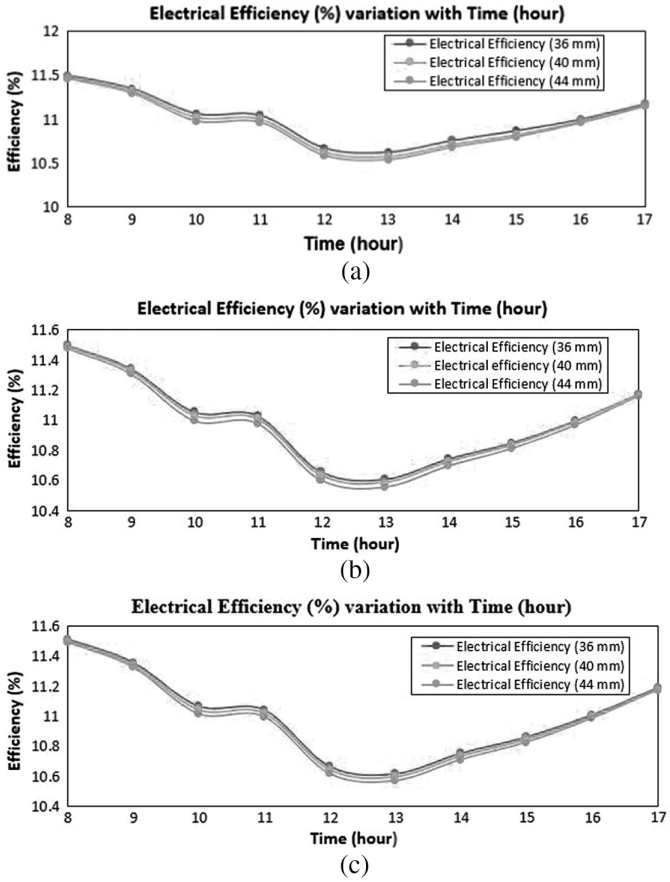

Figure 6. (a) Electrical efficiency variation with time for fixed pitch length ($d = 60$ mm) and varying baffle length (L) 36, 40, and 44 mm and (b) electrical efficiency variation with time for fixed pitch length ($d = 80$ mm) and varying baffle length (L) 36, 40, and 44 mm; and (c) electrical efficiency variation with time for fixed pitch length ($d = 100$ mm) and varying baffle length (L) 36, 40, and 44 mm.

4.3 Overall Efficiency (%) Variation with Time (hour)

Figure 7(a–c) shows the variations of overall efficiency with time for baffle lengths of 36, 40, and 44 mm, respectively, when the pitch length is varied between 60 and 100 mm. From the graphs, it can be seen that the overall efficiency is almost constant during the heating period of the solar collector (*i.e.* from 9 am to 3 pm). In the early morning, the overall efficiency slightly decreases as the sun is low in the sky and in the late afternoon, the same slightly increases due to the increased scattering of solar radiation and glare from the western sky. This trend qualitatively follows the available literature [18].

Irrespective of time and baffle length, thermal efficiency is higher for pitch length of 60 mm corresponding to higher useful heat gain. But, as the pitch length increases, the overall efficiency decreases. And with the increase of baffle length from 36 to 44 mm, the efficiency increases. It follows the same trend of the useful heat gain variation. This trend also qualitatively follows the available literature [17], [18]. The maximum overall efficiency of 44.44% is

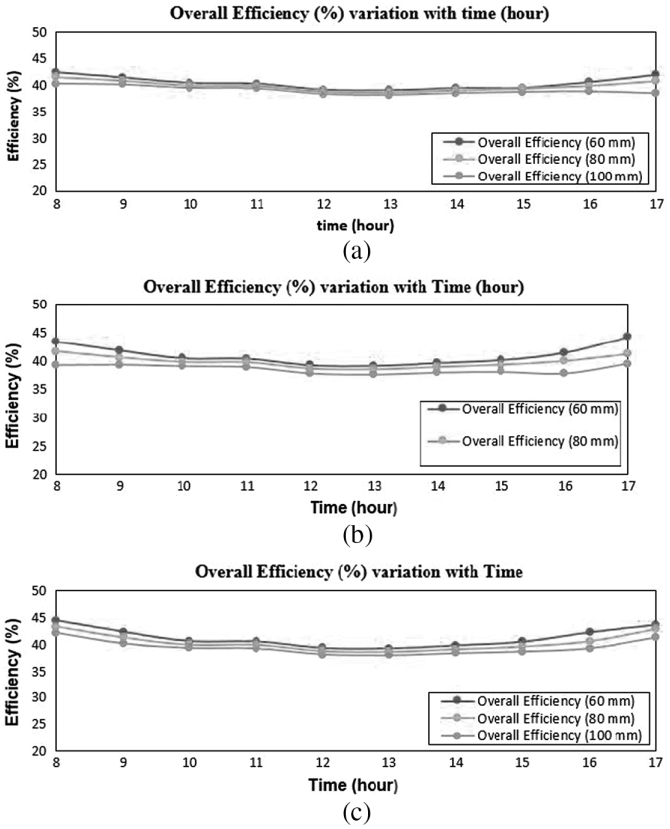

Figure 7. (a) Overall efficiency variation with time for fixed baffle length ($L = 36$ mm) and varying pitch length (d) 60, 80 and 100 mm; (b) overall efficiency variation with time for fixed baffle length ($L = 40$ mm) and varying pitch length (d) 60, 80 and 100 mm; and (c) overall efficiency variation with time for fixed baffle length ($L = 44$ mm) and varying pitch length (d) 60, 80 and 100 mm.

obtained for a baffle length 44 of mm and pitch length of 60 cm.

Last, the flow physics is studied to enumerate the effect of shear-assisted turbulence resulted from the change of heat transfer area due to different pitch lengths, as shown in Fig. 8. It shows the contours of turbulent kinetic energy (m^2/s^2) when the pitch length between two consecutive baffles is increased from 60 to 100 mm for a baffle length of 44 mm. The creator of turbulence is the baffle and shear layers on top of them, as they generate circulation zones inside two consecutive baffles. The contours have been zoomed-in on important portions to show the turbulent kinetic energy distributions. It can be seen how the streamlines coloured by turbulent kinetic energy are generated between the baffles. It can be observed that the concentration of streamlines is increased with increase in pitch length. However, these streamlines are diffused away from the surrounding surfaces in the adjoining area between two consecutive baffles, when the pitch length is more than 60 cm thereby reducing the heat transfer rate from the baffles. This is the reason why the useful heat gain by air and efficiency of the collector decrease with the increase in pitch length.

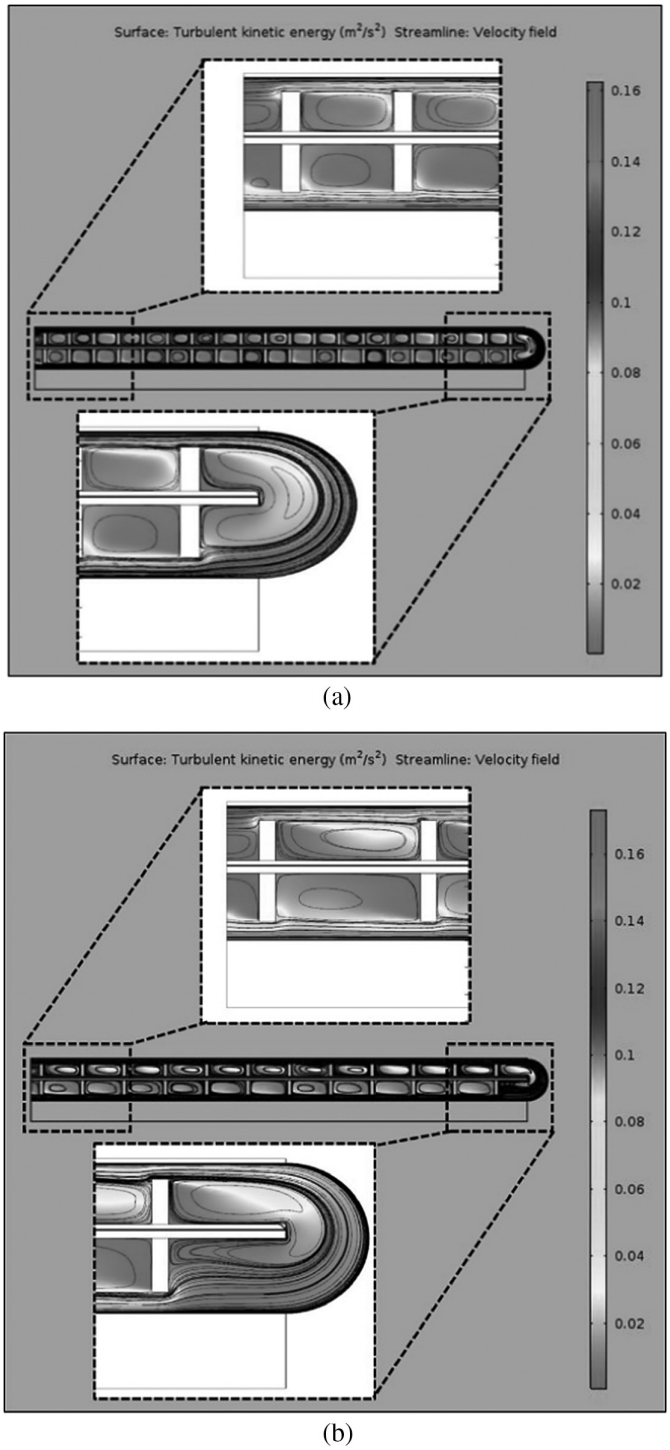

Figure 8. Contours of turbulent kinetic energy for a baffle length of 44 mm and different pitch lengths (a) 60 mm and (b) 100 mm.

4.4 Validation of the Present Model Result

To validate the present CFD model, the works of Hikmet [10] and Hedayatizadeh *et al.* [21] are considered who had investigated the thermal performance of a double-pass solar air heater. Out of the four obstacle designs of the absorber in [10], the best configuration with wavy obstacle is selected. The work of Hedayatizadeh *et al.* [21] considered V-shaped corrugations on the absorber plate of

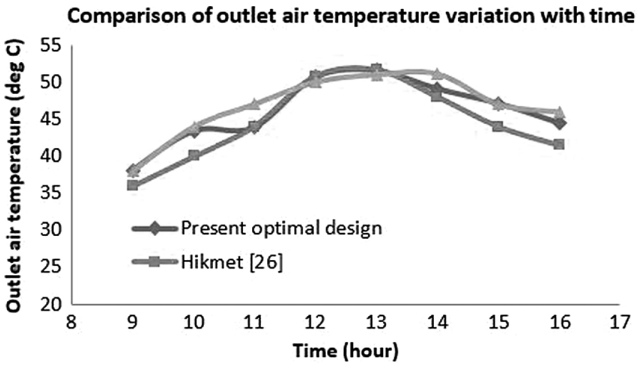

Figure 9. Comparison of outlet temperature variation with literature.

the air collector. Figure 9 shows the comparison of the variations of outlet air temperature with time between the present optimal model design (having a baffle length of 44 mm and a pitch length of 60 mm) with Hikmet design [10] and Hedayatizadeh *et al.* design [21]. The average solar radiation considered in these works is similar to the present work. The figure shows that the present model almost accurately predicts the outlet air temperature compared with the published works on modified absorber design [10], [21], with the maximum air temperature being almost same as the literature result. Moreover, the maximum relative error of reading compared to literature result before and after the noon time is within 9%, which is within the acceptable range.

Some comparisons of the variations of outlet air temperature and electrical efficiency at different time durations between the present study and some literature results are given in Table 5. The corresponding results of Hikmet [10] are also included in the table. Further in this table, the experimental results of electrical efficiency of opaque PV module [22] are included to compare between real solar-electric system with the present PVTC system. In all these works [10], [16]–[18], [22] including the present work, the average solar radiation is around 400 W/m^2. Table 5 clearly shows that the present design has better electrical and thermal performances compared to those benchmark experimental results reported in the literature. Compared to the electrical efficiency of pure PV module, the electrical efficiencies of the PVTC system are higher at all the times (Table 5) except 9:00 and 16:00 h.

5. Conclusion

Following conclusions are drawn:

1. Electrical efficiency of the PVTC becomes maximum (11.51%) when the baffle length is 36 mm and the pitch length is 100 mm.
2. Overall efficiency of the innovative PVTC system is maximum (44.44%) when the baffle length is 44 mm and the pitch length is 60 mm.
3. Larger baffle length (44 mm) and shorter pitch length (60 mm) in the absorber are effective for thermal performance improvement of the PVTC.
4. The performance of the present air-based PVTC design is found better than some literature designs.

Nomenclature

b	baffle width (m)
C_a	specific heat of air (J/Kg·K)
h	heat transfer coefficient (W/m^2·°C)
I	tilted solar radiation (W/m^2)
L	baffle length (m)
L_1	length of absorber plate (m)
$\dot{m}_f$	mass flow rate of air (kg/s)
Q	useful heat gain (W)
T_a	ambient temperature (°C)
$T_{air,out}$	outlet air temperature (°C)
$T_{air,in}$	inlet air temperature (°C)
T_{bs}	bottom surface temperature (°C)
T_c	cell temperature (°C)

Table 5
Comparison of the Variation of Outlet Air Temperature and Electrical Efficiency Between the Present and Literature Results

Time (h)	Outlet Air Temperature (K)			Electrical Efficiency (%)			
	Tiwari *et al.* [16]	Hikmet [10]	Present study	Joshi *et al.* [18]	Tiwari *et al.* [17]	Present study	PV module [22]
9:00 hr	288.50	304.00	311.07	10.6	10.3	11.3	12.2
10:00 hr	296.00	307.50	316.44	10.3	9.80	11.06	11.5
11:00 hr	298.50	319.00	316.88	10.0	9.50	11.04	10.8
12:00 hr	302.00	324.00	323.75	9.9	9.30	10.66	10.3
13:00 hr	303.50	325.00	324.65	9.7	9.40	10.61	10.0
14:00 hr	299.50	319.50	322.16	9.8	9.45	10.75	10.2
15:00 hr	298.00	313.50	320.16	10.1	9.75	10.86	10.7
16:00 hr	296.00	308.00	317.46	10.2	10.25	11.0	11.2

T_f fluid (air) temperature (°C)
U_b bottom heat loss coefficient (from cell to absorber back surface) (W/m^2·°C)
U_t top heat loss coefficient (from cell to ambient) (W/m^2·°C)
dx incremental length of the absorber plate (m)
α_c cell absorptance (%)
α_T absorptance of the thermal collector (%)
β PV cell packing factor (%)
τ_g Glass transmissivity (%)
η_c PV cell efficiency (–)
η_E electrical efficiency (%)
η_o overall efficiency (%)
η_{th} thermal efficiency (%)

Acknowledgement

The authors gratefully acknowledge the support of Regional Test Center and solar PVT laboratory of Mechanical Engineering Department, NIT Silchar.

References

[1] J.C. Mojumder, W.T. Chong, H.W. Ong, K.Y. Leong, and A.A. Mamoon, An experimental investigation on performance analysis of air type photovoltaic thermal collector system integrated with cooling fins design, *Energy Building*, *130*, 2016, 272–285.

[2] N. Dimri, A. Tiwari, and G.N. Tiwari, Thermal modelling of semitransparent photovoltaic thermal (PVT) with thermoelectric cooler (TEC) collector, *Energy Conversion Management*, *146*, 2017, 68–77.

[3] M.E. Slimani-El, M. Amirat, and S. Bahria, Study and modeling of heat transfer and energy performance in a hybrid PV/T collector with double passage of air, *International Journal of Energy for a Clean Environment*, *16*(1–4), 2015, 235–245.

[4] M. Slimani, M. Amirat, I. Kurucz, S. Bahria, A. Hamidat, and W.B. Chaouch, A detailed thermal-electrical model of three photovoltaic/thermal (PV/T) hybrid air collectors and photovoltaic (PV) module: Comparative study under Algiers climatic conditions, *Energy Conversion Management*, *133*, 2017, 458–476.

[5] P. Velmurugan and R. Kalaivanan, Thermal performance studies on multi-pass flat-plate solar air heater with longitudinal fins: An analytical approach, *Arabian Journal of Science and Engineering*, *40*(4) , 2015, 1141–1150.

[6] P. Velmurugan and R. Kalaivanan, Energy and exergy analysis of solar air heaters with varied geometries, *Arabian Journal of Science and Engineering*, *40*(4), 2015, 1173–1186.

[7] E. Cuce and P.M. Cuce, Tilt angle optimization and passive cooling of Building-Integrated Photovoltaics (BIPVs) for better electrical performance, *Arabian Journal of Science and Engineering*, *39*(11), 2014, 8199–8270.

[8] N.K. Pandey, V.K. Bajpai, and Varun, Heat transfer and friction factor study of a solar air heater having multiple arcs with gap-shaped roughness element on absorber plate, *Arabian Journal of Science and Engineering*, *44*(11), 2016, 4517–4530.

[9] M. Abuşka and M.B. Akgl, Experimental study on thermal performance of a novel solar air collector having conical springs on absorber plate, *Arabian Journal of Science and Engineering*, *44*(11), 2016, 4509–4516.

[10] E. Hikmet, Experimental energy and exergy analysis of a double-flow solar air heater having different obstacles on absorber plates, *Building and Environment*, *43*, 2008, 1046–1054.

[11] K. Touafek, A. Khelifa, H. Haloui, H.B.C. El Hocine, L. Boutina, M.T. Baissi, S. Haddad, and I. Tabet, Improvement of performances of solar photovoltaic/thermal air collector in South Algeria, *2018 6th International Renewable and Sustainable Energy Conference (IRSEC)*, Rabat, Morocco, 5–8 December 2018.

[12] J.C. Mojumder, W.T. Chong, H.C. Ong, K.Y. Leong, and A. Mamoon, An experimental investigation on performance analysis of air type photovoltaic thermal collector system integrated with cooling fins design, *Energy and Buildings*, *130*, 2016, 272–285.

[13] J. Hu and G. Zhang, Performance improvement of solar air collector based on airflow reorganization: A review, *Applied Thermal Engineering*, *155*, 2019, 592–611.

[14] S. Diwania, S. Agrawal, A.S. Siddiqui, and S. Singh, Photovoltaic–thermal (PV/T) technology: A comprehensive review on applications and its advancement, *International Journal of Energy and Environmental Engineering*, *11*, 2020, 33–54.

[15] M. Chandrasekar, S. Suresh, and T. Senthilkumar, Passive cooling of standalone flat PV module with cotton wick structures, *Energy Conversion and Management*, *71,* 2013, 43–50.

[16] A. Tiwari, M.S. Sodha, A. Chandra, and J.C. Joshi, Performance evaluation of photovoltaic thermal solar air collector for composite climate of India, *Solar Energy Materials & Solar Cells*, *90*, 2006, 175–189.

[17] G. Tiwari, R. Mishra, and S. Solanki, Photovoltaic modules and their applications: A review on thermal modelling, *Applied Energy*, *88*, 2011, 2287–2304.

[18] A. Joshi, A. Tiwari, G. Tiwari, I. Dincer, and B.V. Reddy, Performance evaluation of a hybrid photo voltaic thermal (PV/T) (glass-to-glass) system, *International Journal of Thermal Sciences*, *48*, 2009, 154–164.

[19] R.K. Mishra and G. Tiwari, Evaluation of an integrated photovoltaic thermal solar (IPVTS) water heating system for various configurations at constant collection temperature, *World Renewable Energy Congress, Linkoping* (Sweden: Citeseer, 2011), 3749–3756.

[20] S. Dubey, S. Solanki, and A. Tiwari, Energy and exergy analysis of PV/T air collectors connected in series, *Energy and Buildings*, *41*, 2009, 863–870.

[21] M. Hedayatizadeh, F. Sarhaddi, A. Safavinejad, F. Ranjbar, and H. Chaji, Exergy loss-based efficiency optimization of a double-pass/glazed v-corrugated plate solar air heater, *Energy*, *94*, 2016, 799–810.

[22] A. Gaur and G.N. Tiwari, Performance of photovoltaic modules of different solar cells, *Journal of Solar Energy*, *2013*, 2013, Article ID 734581.

Biographies

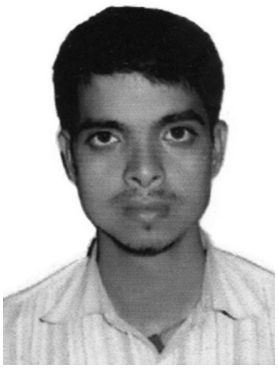

Sanjeet Kumar completed undergraduate degree from Hooghly Engineering & Technology College, West Bengal, India, in mechanical engineering in 2016 and completed the postgraduate degree from NIT Silchar, Assam, India, in thermal engineering in 2018. His research interest includes solar air heating collector and solar thermal systems in general.

Supreme Das is a research scholar in the Department of Mechanical Engineering, NIT Silchar. He has over four years of experience in teaching and has been involved in research work in the domain of renewable energy since 2018. His areas of interest include experimental and CFD applications in the field of solar energy.

Dr. Agnimitra Biswas did his B.E. in Mechanical Engineering from Regional Engineering College Silchar in 2001, M. Tech. in Thermal Engineering from NIT Silchar in 2007, and Ph.D. in Mechanical Engineering from NIT Silchar in 2010. His research area was Vertical Axis Wind Turbines using experimental and computational methods. He has more than 13 years of teaching and research experiences. Presently, he is working as an Assistant Professor in ME Department, NIT Silchar since November 2012. His current research areas include hybrid renewable energy systems, vertical axis wind turbines, micro hydro-turbines, and solar energy systems. He has published more than 60 research papers till date in various refereed international journals and conferences. He is an associate member of Institution of Engineers (India). He is a regular reviewer of various Energy-related SCI indexed journals. He is also the principal investigator of Ministry of New & Renewable Energy (MNRE) sponsored solar RTC project of this institution, and an in-charge of MNRE recognized Regional Test Center for solar thermal devices at ME Department, NIT Silchar. This centre has bagged the prestigious NABL accreditation for testing laboratory in 2017.

Dr. Biplab Das presently working as Assistant Professor in the Department of Mechanical Engineering, National Institute of Technology Silchar, India. Dr. Das completed his Ph.D. from NERIST, Itanagar, India, in the year of 2014. Later, he pursued his Post-Doctoral research from University of Idaho, USA. He is the recipient of prestigious Bhaskara Advance Solar Energy (BASE) fellowship from IUSSTF and DST, Govt. of India. He is also awarded with "DBT Associateship" by Department of Biotechnology, Government of India. He has 12+ years of experience in teaching and research, and published 40+ refereed journal papers. He has guided 3 Ph.D. students and more than 8 nos. of Ph.D. scholars who are pursuing Ph.D. Dr. Das is a reviewer of 20+ reputed journals of Elsevier, ASME, Springer, *etc.*, and Guest Editor (special issue) of two journals of Advances in Mechanical Engineering and Entropy.